nature medicine

House dust mite allergen induces asthma via Toll-like receptor 4 triggering of airway structural cells

Hamida Hammad[1,4], Marcello Chieppa[2,4], Frederic Perros[1], Monique A Willart[1], Ronald N Germain[2] & Bart N Lambrecht[1,3]

© 2009 Nature America, Inc. All rights reserved.

Barrier epithelial cells and airway dendritic cells (DCs) make up the first line of defense against inhaled substances such as house dust mite (HDM) allergen and endotoxin (lipopolysaccharide, LPS). We hypothesized that these cells need to communicate with each other to cause allergic disease. We show in irradiated chimeric mice that Toll-like receptor 4 (TLR4) expression on radioresistant lung structural cells, but not on DCs, is necessary and sufficient for DC activation in the lung and for priming of effector T helper responses to HDM. TLR4 triggering on structural cells caused production of the innate proallergic cytokines thymic stromal lymphopoietin, granulocyte-macrophage colony–stimulating factor, interleukin-25 and interleukin-33. The absence of TLR4 on structural cells, but not on hematopoietic cells, abolished HDM-driven allergic airway inflammation. Finally, inhalation of a TLR4 antagonist to target exposed epithelial cells suppressed the salient features of asthma, including bronchial hyperreactivity. Our data identify an innate immune function of airway epithelial cells that drives allergic inflammation via activation of mucosal DCs.

Aberrant innate and adaptive immune responses to allergens and environmental pollutants lead to respiratory disease, including asthma and chronic obstructive pulmonary disease[1]. Airway DCs continuously sample inhaled air for the presence of noxious substances via cellular processes that extend across the airway mucosal barrier[2]. By simultaneously expressing pattern recognition receptors such as the TLRs to sense the presence of pathogens, and by presenting pathogen-derived antigens to naive T cells in the lymph nodes, DCs bridge innate and adaptive immunity. An emerging theme in the field of lung immunology is that structural cells of the airways such as epithelial cells, endothelial cells, fibroblasts and other stromal cells produce activating cytokines that determine the quantity and quality of the lung immune response[3–8]. For example, barrier epithelial cells make up the first line of defense against inhaled antigens and also express TLRs[9,10], allowing them to sense the same types of stimuli that are recognized by innate immune cells. A major issue that remains to be elucidated is the precise contribution of epithelial TLR triggering to the DC-driven adaptive immune response. Here we address this issue by studying key aspects of airway DC biology after inhalation of the TLR4 ligand LPS, found predominantly in the wall of Gram-negative organisms, as well as after inhalation of HDM, a ubiquitous indoor allergen contaminated with LPS from colonizing bacteria and environmental pollution[11]. We generated radiation-chimeric mice in which either radioresistant structural cells or radiosensitive hematopoietic cells (including DCs) were deficient in TLR4 expression, and we show that TLR4 expression on structural cells is necessary and sufficient for activation of immune responses by mucosal DCs and development of T helper type 2 (T_H2) immunity and allergic inflammation to HDM allergen.

RESULTS

TLR4 on radioresistant cells controls innate immunity to LPS

To determine the relative contribution of TLR4 signaling on lung structural cells versus hematopoietic cells in the innate immune response to inhaled LPS, we generated radiation-induced chimeric mice (**Fig. 1a**). In WT→WT mice (where WT bone marrow was injected into irradiated WT recipients), we found TLR4 expression predominantly on airway epithelial cells and alveolar macrophages, whereas in *Tlr4*$^{-/-}$→WT mice expression was restricted to epithelial cells and in WT→*Tlr4*$^{-/-}$ mice expression was mainly found on alveolar macrophages (**Fig. 1b**). Twelve weeks after reconstitution, chimerism was confirmed by flow cytometry in lymph node B cells, DCs and autofluorescent alveolar macrophages (**Fig. 1c**).

First, we examined the cellular influx into the lung after an intratracheal (i.t.) administration of LPS. WT→WT mice exposed to LPS had more Ly-6G^{hi} CD11b^{+} neutrophils (**Fig. 2a**) and Ly6C^{hi} CD11b^{+} monocytes (**Fig. 2b**) in the lungs than did mice given PBS, but this response was markedly reduced in *Tlr4*$^{-/-}$→*Tlr4*$^{-/-}$ mice (**Fig. 2b**). Expression of TLR4 on structural cells was crucial, as WT→*Tlr4*$^{-/-}$ mice failed to recruit neutrophils and monocytes in response to LPS (**Fig. 2b**). Neutrophil, but not monocyte, numbers were also slightly lower in *Tlr4*$^{-/-}$→WT mice as compared to WT→WT mice

[1]Laboratory of Immunoregulation and Mucosal Immunology, Department of Respiratory Medicine, Ghent University, Ghent, Belgium. [2]Laboratory of Immunology, Section of Lymphocyte Biology, National Institute of Allergy and Infectious Diseases, US National Institutes of Health, Bethesda, Maryland, USA. [3]Department of Pulmonary Medicine, Erasmus University Medical Center, Rotterdam, The Netherlands. [4]These authors contributed equally to this work. Correspondence should be addressed to B.N.L. (bart.lambrecht@ugent.be).

Received 17 September 2008; accepted 26 February 2009; published online 29 March 2008; doi:10.1038/nm.1946

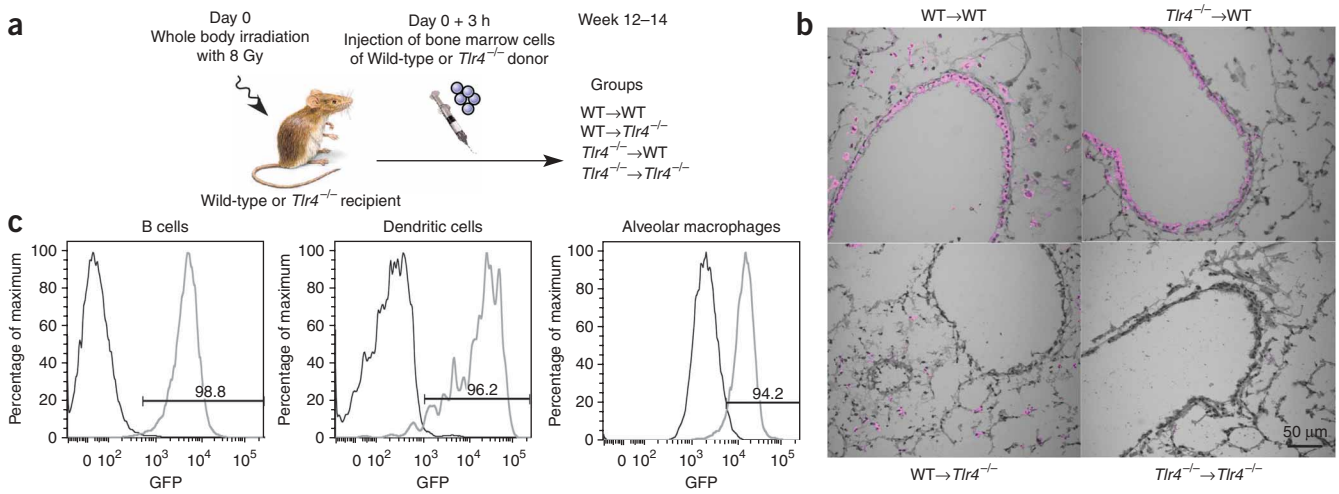

Figure 1 Assessment of the reconstitution rate of chimeric mice. (**a**) Schematic of chimeric mice preparation (denoted as bone marrow donor genotype→recipient genotype). (**b**) TLR4 expression in the airways of the diverse chimeric mice, as assessed by immunostaining and confocal imaging (purple). This image was merged with a bright-field image. (**c**) The percentage of GFP+ B cells and DCs in lymph node and alveolar macrophages of $WT^{MHCIIgfp}$→WT mice (gray histogram). The background for GFP positivity was set on fluorescence intensity of mice receiving GFP-negative bone marrow (black histogram). These experiments were done three times.

exposed to LPS (**Fig. 2b**). To determine the mechanism behind the decrease in cellular recruitment in mice lacking TLR4 expression on structural cells, we measured the lung concentrations of relevant chemokines. After the administration of LPS, WT→WT mice showed a substantial increase in the concentrations of several chemokines and growth factors for neutrophils (KC, **Fig. 2c**; granulocyte colony–stimulating factor, **Supplementary Fig. 1** online) and for monocytes and DCs (C-C chemokine ligand-2 (CCL2), **Fig. 2d**; CCL20, **Supplementary Fig. 1**), compared to mice given PBS. These responses were largely abolished in *Tlr4*$^{-/-}$→*Tlr4*$^{-/-}$ or WT→*Tlr4*$^{-/-}$ chimeras given LPS, yet they were intact in *Tlr4*$^{-/-}$→WT chimeras (**Fig. 2c,d** and **Supplementary Fig. 1e**).

As part of innate immunity to microbial triggers, DCs are recruited to the lung. The number of major histocompatibility complex class II (MHCII)-positive $CD11c^{hi}$ DCs in the trachea was markedly increased by LPS administration in WT→WT mice (**Fig. 2e**). In WT→*Tlr4*$^{-/-}$ and *Tlr4*$^{-/-}$→*Tlr4*$^{-/-}$ chimeras, DC recruitment in response to LPS was substantially lower (**Fig. 2e**). In PBS-injected WT→WT mice, the majority of $CD11c^{hi}$ DCs in the trachea were CD11b negative, whereas in LPS-injected mice, there was accumulation of an inflammatory $CD11b^{hi}$ DC subset, an effect not seen in WT→*Tlr4*$^{-/-}$ or *Tlr4*$^{-/-}$→*Tlr4*$^{-/-}$ chimeras but maintained in *Tlr4*$^{-/-}$→WT mice (**Fig. 2f**). As an additional control, we administered the TLR2 ligand peptidoglycan and found that responses to this compound were not affected by TLR4 deficiency on stromal cells (**Supplementary Fig. 1**).

Figure 2 TLR4 expression on radioresistant stromal cells is necessary and sufficient for recruitment of DCs to the lungs in response to LPS. (**a**–**f**) Chimeric mice were injected i.t. with LPS or PBS and analyzed 24 h later. (**a**) Quantification of BAL fluid neutrophils. (**b**) Quantification of BAL fluid monocytes. (**c**,**d**) Quantification of KC chemokine production involved in the recruitment of neutrophils (**c**) and CCL2 production for monocytes and DCs (**d**) in BAL fluids. (**e**) Quantification of tracheal digest $MHCII^+CD11c^+$ dendritic cells. (**f**) Quantification of $MHCII^+CD11c^+CD11b^+$ DCs. The tracheal counts have been corrected for 1×10^6 $CD45^{neg}$ structural cells to correct for differently sized explants. $^*P < 0.05$. This is a representative experiment out of four. Four to six mice were used per group.

TLR4 on radioresistant cells determines dynamic DC behavior

As part of their normal physiology, DCs residing in the periphery scan the environment for incoming antigen. We therefore used two-photon dynamic imaging to evaluate the behavior of MHCII-$EGFP^+$ DCs (DCs genetically tagged with enhanced green fluorescent protein (EGFP) expressed from the MHC class II locus) in freshly isolated tracheal explants from chimeric mice exposed to LPS. To exclude the presence of contaminating $MHCII^+$ B cells also known to be found in the conducting airways of rodents, we generated chimeras using donor mice deficient in both Rag1 and Rag2 and expressing MHCII-EGFP. As soon as 2 h after *in vivo* administration of LPS to WT→WT chimeras, there was a massive recruitment of DCs to the trachea, an effect not seen in PBS-treated or LPS-exposed WT→*Tlr4*$^{-/-}$ mice (**Fig. 3a**) The few DCs in the trachea of WT→WT chimeras given PBS made only small lateral movements (**Supplementary Movie 1** online), whereas after administration of LPS DCs showed an increased velocity and made rapid lateral movements (movements quantified in **Supplementary Fig. 2** online).

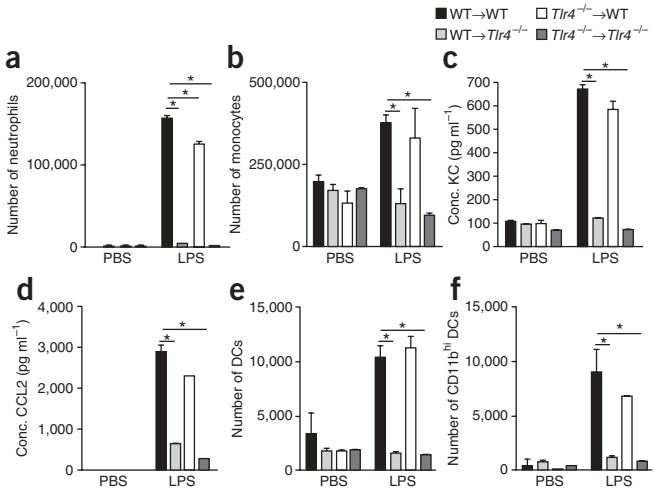

© 2009 Nature America, Inc. All rights reserved.

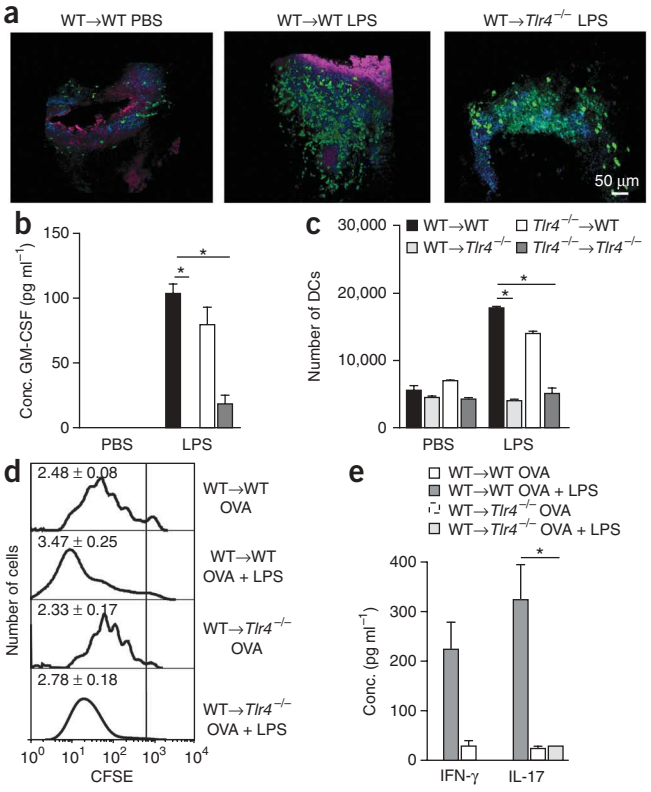

Figure 3 TLR4 expression on radioresistant stromal cells is necessary and sufficient for activation of mucosal DCs. (**a**) Two-photon microscopy of tracheal explants from WT→WT and WT→*Tlr4*$^{-/-}$ chimeras 2 h after i.t. injection with LPS or PBS. Green DCs are located within the epithelial layer. Nuclei were counterstained in blue. (**b**) GM-CSF concentration in BAL fluids was measured 24 h after LPS exposure. (**c**) Number of OVA^{+} migrating DCs was enumerated in the MLNs 36 h after chimeric mice were injected i.t. with fluorescent OVA^{AF647} together with LPS or PBS. (**d**) T cell proliferation in the MLNs at day 5 after WT→WT and WT→*Tlr4*$^{-/-}$ chimeras received an intravenous injection of CFSE-labeled OVA-specific naive OTII T cells and were given OVA and LPS or OVA and PBS i.t. on day 1. The proliferation index for each group is shown in the upper right corner of the histograms. (**e**) Cytokine production by MLN cells 5 d after OVA and LPS administration. $^{*}P < 0.05$. These panels show one representative experiment out of two to four experiments with four to six mice per group.

Some DCs also migrated toward and away from the epithelium (**Supplementary Movie 2** online). However, when LPS was administered to WT→*Tlr4*$^{-/-}$ chimeras, the majority of DCs from the trachea showed the same sessile behavior as DCs in PBS-injected mice (**Supplementary Movie 3** online).

TLR4 on radioresistant cells determines DC maturation

To determine to what extent structural cell–driven inflammation affects phenotypic maturation of DCs, we examined the expression of co-stimulatory molecules on airway DCs. After LPS instillation, airway DCs from WT→WT and *Tlr4*$^{-/-}$→WT chimeras showed more than threefold increased expression of CD86 and CD40 when compared with PBS controls, but this response was selectively abolished in WT→*Tlr4*$^{-/-}$ and *Tlr4*$^{-/-}$→*Tlr4*$^{-/-}$ mice (**Supplementary Table 1** online). We observed similar results when we studied DCs from digested lung and mediastinal lymph node (MLN) DCs (data not shown). To determine the basis for the failure of phenotypic DC maturation in WT→*Tlr4*$^{-/-}$ chimeras, we measured the lung concentrations of several DC-activating cytokines, including granulocyte-macrophage colony–stimulating factor (GM-CSF), interlukin-1β (IL-1β) and thymic stromal-derived lymphopoietin (TSLP). Although we could not detect any production of TSLP, the administration of LPS induced higher production of GM-CSF (and IL-1β, data not shown) in the BAL of WT→WT and *Tlr4*$^{-/-}$→WT chimeras, an effect not seen in WT→*Tlr4*$^{-/-}$ and *Tlr4*$^{-/-}$→*Tlr4*$^{-/-}$ chimeras (**Fig. 3b**).

As part of their maturation, activated DCs migrate to the draining MLNs[8]. Therefore, we gave mice fluorescently labeled ovalbumin (OVA^{AF647}) i.t. together with LPS or PBS, and we enumerated OVA^{AF647+}MHCII^{hi}CD11c^{hi} migrating DCs in the MLNs[2]. LPS administration into WT→WT chimeras strongly increased the number of OVA^{+} DCs to the MLNs compared to PBS, but this response was significantly reduced in WT→*Tlr4*$^{-/-}$ and *Tlr4*$^{-/-}$→*Tlr4*$^{-/-}$ chimeras, and it was intact in *Tlr4*$^{-/-}$→WT chimeras (**Fig. 3c**).

The phenotypic changes observed in pathogen-associated molecular pattern–activated DCs usually—but not always—correlate with an increased capacity of the cells to stimulate antigen-driven T cell proliferation and differentiation[12]. To examine this issue in the present model system, we gave chimeric mice OVA-specific naive CD4^{+} T cells and subsequently immunized them by i.t. injection of OVA in combination with LPS (OVA-LPS) or control PBS (OVA-PBS). In WT→WT chimeras, OVA-PBS induced vigorous proliferation of naive CD4^{+} T cells in the MLNs, and this response was further increased by co-injection of LPS (**Fig. 3d**). Notably, T cell proliferation was lower in WT→*Tlr4*$^{-/-}$ chimeras injected with OVA-LPS compared with WT→WT mice, although not to the degree seen in mice given OVA-PBS (**Fig. 3d**).

We next evaluated the amounts of the prototypical T_H1, T_H2 and T_H17 cytokines (interferon-γ (IFN-γ), IL-5 and IL-17, respectively) produced by MLN cells. Very low concentrations of IL-17 and IFN-γ were present in the supernatants of MLN cultures from

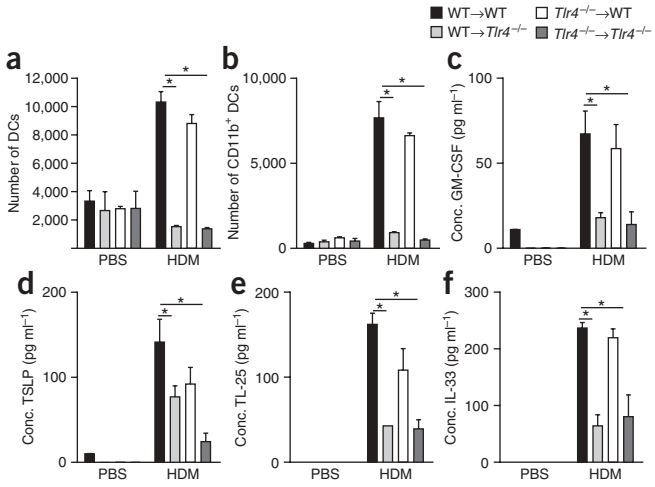

Figure 4 TLR4 expression on airway structural cells is necessary and sufficient for an innate immune response to HDM allergen. (**a**,**b**) MHCII^{+}CD11c^{+} (**a**) MHCII^{+}CD11c^{+}CD11b^{+} (**b**) DC counts in tracheal digests 24 h after chimeras were injected i.t. with PBS or HDM allergen. The tracheal counts have been corrected for 1×10^{6} CD45^{-} structural cells to correct for differently sized explants. (**c**–**f**) Production of GM-CSF (**c**), TSLP (**d**), IL-25 (**e**) and IL-33 (**f**) in BAL fluids. $^{*}P < 0.05$. This is one representative experiment out of three. Five or six mice were used per group.

© 2009 Nature America, Inc. All rights reserved.

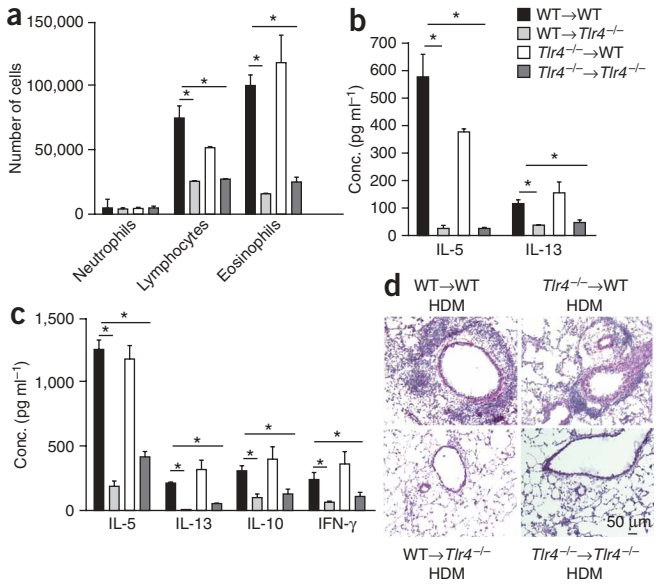

Figure 5 TLR4 expression on airway structural cells is necessary and sufficient for HDM-driven T_H2 responses and allergic inflammation. Chimeras were injected i.t. with HDM allergen on days 0, 7 and 14. (**a**) Quantification of neutrophils, lymphocytes and eosinophils in BAL fluid 72 h after challenge, as analyzed by flow cytometry. (**b**) Cytokine concentrations in BAL fluids. (**c**) Cytokine concentrations in MLN cells re-stimulated *in vitro* for 5 d with 30mg ml^{-1} HDM. (**d**) H&E staining of lung sections. These experiments were performed two times with four to six mice per group. One representative experiment is shown.

OVA-PBS–injected mice (**Fig. 3e**). In WT→WT mice exposed to OVA-LPS, the concentrations of IL-17 and IFN-γ were increased compared to mice exposed to OVA-PBS, an effect not seen in WT→*Tlr4*$^{-/-}$ chimeras (**Fig. 3e**). No IL-5 production was detected in any of the supernatants tested (data not shown). The unavailability of T cell receptor–transgenic T cells on a *Tlr4*$^{-/-}$ background did not allow us to perform the opposite experiment (*Tlr4*$^{-/-}$→ WT).

Tlr4 on radioresistant cells determines T_H2 immunity to HDM

We next investigated the importance of *Tlr4* expression on structural cells in the innate response to complex and relevant allergens such as HDM extracts, which are known also to contain large amounts of LPS[11,13]. The HDM extract contained 1.05 ng LPS per mg extract. HDM administration (100 μg) in the airways of WT→WT and *Tlr4*$^{-/-}$→WT mice resulted in an increase in monocyte (data not shown) and DC (**Fig. 4a,b**) numbers in the airways and an increase in CCL2 and CCL3 concentration in the bronchoalveolar lavage (BAL) fluid (**Supplementary Fig. 3** online) compared with PBS administration, responses that were markedly lower in *Tlr4*$^{-/-}$→*Tlr4*$^{-/-}$ and WT→*Tlr4*$^{-/-}$ mice. There was no induction of KC or G-CSF, and, consequently, airway neutrophilia did not develop (data not shown).

Because the administration of HDM in the airways is known to induce T_H2 responses in the lungs[14–16], we evaluated the production of cytokines known to promote eosinophilic inflammation[17–19]. The concentrations of GM-CSF, TSLP, IL-25 and IL-33 were markedly increased in the BAL fluids of WT→WT mice exposed to a single administration of HDM compared with mice injected with PBS (**Fig. 4c–f**). For comparison, some mice were also injected with a low (100 ng) and high (10 μg) dose of endotoxin, which has been previously shown to induce T_H2 and T_H1 immunity, respectively[20]. Whereas both doses of LPS and HDM were able to induce IL-33 production, production of TSLP and IL-25 was induced only by HDM (**Supplementary Fig. 4** online). This innate cytokine response to HDM was lower in WT→*Tlr4*$^{-/-}$ and *Tlr4*$^{-/-}$→*Tlr4*$^{-/-}$ chimeras, yet maintained in *Tlr4*$^{-/-}$→WT mice, although there was a trend for reduced TSLP production in the latter mice (**Fig. 4d**).

We next examined the influence of TLR4 deficiency in structural versus hematopoietic cells on allergic inflammation induced by repeated i.t. injection of HDM extracts[14]. WT→WT chimeric mice developed T_H2-associated airway inflammation characterized by BAL fluid and bronchovascular lymphocytosis, eosinophilia and goblet cell hyperplasia (**Fig. 5**). These are features of a T_H2 response, consistent with high concentrations of IL-5 and IL-13 in the BAL fluid (**Fig. 5b**) and in cultures of MLN lymphocytes re-stimulated with HDM *in vitro*

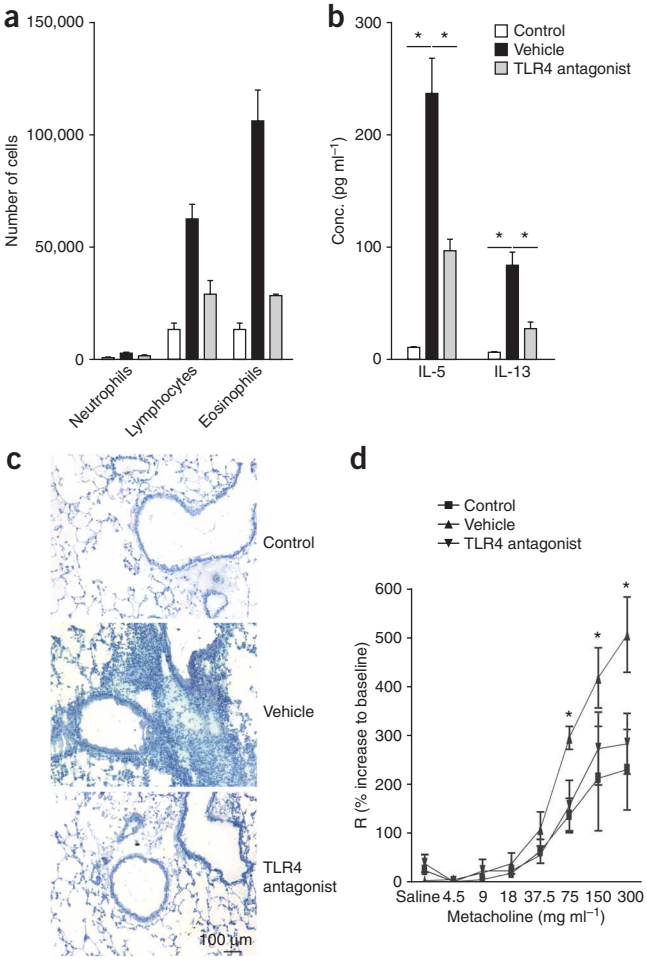

Figure 6 Intrapulmonary delivery of a TLR4 antagonist reduces HDM-driven inflammation and airway hyper-responsiveness. C57BL/6 mice were exposed to HDM or to PBS (control) on day 0. All of the mice were then challenged with HDM admixed to a TLR4 antagonist or the vehicle on days 7 and 14. (**a**) Differential cell count of BAL fluid, as determined by flow cytometry 72 h after challenge. (**b**) Cytokine concentrations in BAL fluids. (**c**) Hematoxylin staining of lung sections. (**d**) Lung function, as determined by invasive measurement of airway resistance (R) in response to increasing concentrations of metacholine. $^*P < 0.05$. These experiments were performed two times with six mice per group. One representative experiment is shown.

© 2009 Nature America, Inc. All rights reserved.

(**Fig. 5c**). All of these features of allergic inflammation were severely reduced in WT→*Tlr4*$^{-/-}$ and *Tlr4*$^{-/-}$→*Tlr4*$^{-/-}$ chimeras, yet maintained in *Tlr4*$^{-/-}$→WT mice (**Fig. 5a–d**).

Inhalation of TLR4 antagonist reduces asthma features

On the basis of these data and on the fact that TLR4 was mainly expressed on exposed conducting airway epithelial cells (**Fig. 1**), we hypothesized that local intrapulmonary administration of a TLR4 antagonist might constitute a unique therapeutic strategy for allergic inflammation. Administration of an underacylated form of *Rhodobacter sphaeroides* LPS (behaving as a functional TLR4 antagonist) at the time of HDM injections strongly reduced airway lymphocytosis and eosinophilia down to the level of control nonsensitized mice, compared with vehicle-treated mice (**Fig. 6a**). This was accompanied by a marked reduction in IL-5 and IL-13 concentrations in the BAL fluid (**Fig. 6b**). Tissue histology showed that TLR4 antagonist treatment decreased the peribronchovascular infiltrates and goblet cell hyperplasia (**Fig. 6c**). Finally, TLR4 antagonist suppressed the invasively measured airway hyper-responsiveness to the bronchoconstrictor metacholine seen in actively sensitized mice to the level seen in control sham-sensitized mice (**Fig. 6d**).

DISCUSSION

It has recently been shown that TLR4 stimulation of radioresistant structural cells of the spleen is neither required nor sufficient to induce functional splenic DC maturation in response to systemically administered LPS[21]. In contrast, our study shows that TLR4 triggering on lung structural cells by LPS and HDM is required and sufficient to activate many aspects of the functional behavior of mucosal DCs in response to LPS inhalation. Of all the radioresistant structural cells, epithelial cells that line the airways are the most likely to mediate the effects of LPS, given their exposed position, their known[9] and confirmed (**Fig. 1**) expression of TLR4 and their activation of TLR-dependent signaling cascades upon exposure to TLR ligands[6,7,22–24].

The number of airway DCs increased over the resting state after LPS and HDM exposure, most likely owing to production of DC-attractive chemokines by epithelial cells. The chemokine CCL20, produced by activated airway epithelial cells[5,25], is known to attract CCR6^{+} human lung DCs and was found to be produced in a TLR4-dependent manner. Production of CCL20 also occurs when human bronchial epithelial cell lines are exposed to HDM in a pathway requiring recognition of β-glucans but not endotoxin[26]. Upregulation of the CCL2-CCR2 axis is a more credible explanation for the increase in DCs, as CCR2^{+}Ly6c^{hi} monocytes are precursors to CD11b^{+} inflammatory DCs, and we observed a clear increase in these cells as well as the CCL2 ligand in the airways after LPS and HDM challenge[27,28]. During acute allergen challenge in the OVA model, CCR2 and not CCR6 was found to control inflammatory DC chemotaxis to the lung[27].

Another paradigmatic feature of resident and freshly recruited DCs is their potential to scan the environment for incoming antigen. By live imaging of freshly explanted tracheal samples, we observed that LPS and HDM (data not shown) inhalation induced a rapid scanning behavior of DCs that depended on TLR4 expression by structural cells. Although we do not yet fully understand the contribution of these rapid lateral movements to uptake of airway luminal contents, we propose that they are necessary for DCs to find antigen efficiently in this anatomical site. How this chemokinetic behavior is induced, and which stromal-derived factors are involved in this phenomenon, remain unclear, but the process might involve the radioresistant unmyelinated nervous system that closely coincides with DC processes[29]. Alternatively, the chemokines may adhere to glycoaminoglycans in the airway lumen and constitute a solid-phase matrix that evokes the migratory response, similar to that proposed for chemokines bound to fibroblastic reticular cells in the lymph nodes[30].

Once activated in the airways, DCs migrate in a CCR7-dependent way to the T cell area of draining MLNs[31], and our data using LPS or HDM show that this behavior depends on TLR4 expression on structural cells. Whether this decreased migration of DCs to MLNs in *Tlr4*$^{-/-}$ mice is due to the absence of signals released from activated stromal cells, or whether it is just a reflection of the immature state of airway DCs in these chimeras, still needs to be elucidated. DC activation, as read out by CD86 and CD40 expression, was clearly reduced in the absence of TLR4 triggering, most likely as a result of decreased production of DC maturation cytokines such as GM-CSF[32,33]. Once migrating DCs arrive in the lymph node, they induce T cell activation as part of their maturation program[12]. Although signals derived from TLR4 triggering on structural cells were not required for DC-driven antigen-specific T cell proliferation, they were crucial for induction of effector T_H1 and T_H17 responses to OVA mixed with LPS and a T_H2 response to HDM allergen. The fact that T cell proliferation of WT→*Tlr4*$^{-/-}$ chimeras exposed to OVA and LPS was higher than that seen in those given OVA alone argues that, in addition to signaling on structural cells, there is also direct recognition of LPS by airway DCs that might be crucial for inducing effector potential in OVA-specific T cells. Other researchers have suggested that lung DCs directly react to OVA contaminated with LPS in an myeloid differentiation protein-88–dependent way[20,34]. However, experiments in *Tlr4*$^{-/-}$→WT chimeras exposed to the real-life antigen HDM revealed that TLR4 expression on stromal cells alone is sufficient to induce T_H2 effector potential in T cells. The concerted effects of mediators derived from both DCs and stromal cells might be required in synergy to optimally induce effector T cell immunity to a harmless antigen like OVA, as opposed to one like HDM that contains enzymes known to activate epithelial cells and basophils[8].

Finally, we addressed whether absence of TLR4 from stromal cells would affect allergic responses to HDM. HDM extract contains endotoxin, and its levels in house dust have been correlated with a modifying effect on allergic sensitization in children[13]. It has been proposed that low-dose endotoxin promotes T_H2 immunity, whereas high-dose promotes T_H1 responses[20]. To our surprise, the degree of endotoxin contamination of HDM extract was in the subnanogram range, far below the dose previously used to promote T_H2 responses to OVA[20]. The innate cytokine immune response to HDM extract (as determined by GM-CSF, TSLP, IL25 and IL-33 concentrations) was profoundly altered when TLR4 was absent on structural cells, suggesting a major role for this low level of contaminating LPS. However, this cytokine response cannot be entirely due to the LPS contaminating HDM, as giving LPS alone induced a profoundly different response compared to HDM administration. Recently, the Der p 2 allergen was found to enhance the response of mouse bronchial epithelial cells to endotoxin by acting as an MD2-like chaperone that promotes TLR4 signaling[11]. It will be useful to study whether this MD2-like effect of Der p 2 not only enhances but also alters the type of innate immune response induced by endotoxin in the airways, as it might explain the profound proallergic innate response to HDM.

A failure to produce these innate cytokines in *Tlr4*$^{-/-}$ mice might explain how HDM allergy is avoided. GM-CSF promotes DC maturation and breaks inhalation tolerance[3]. TSLP is produced by epithelial cells, mast cells and basophils and activates DCs and mast cells[19,35–37]. IL-25 is made by mast cells, basophils, eosinophils and epithelial cells

© 2009 Nature America, Inc. All rights reserved.

and boosts T_H2 cytokine production[36]. IL-33 boosts T_H2 cytokine production and promotes goblet cell hyperplasia[18,38]. The induction of these cytokines in BAL fluid strongly depends on structural TLR4 expression, most likely reflecting production by epithelial cells. Not unexpectedly, when we exposed WT → *Tlr4*$^{-/-}$ mice to repeated HDM aerosols, they failed to develop the salient features of allergic inflammation such as airway eosinophilia, goblet cell hyperplasia and peribronchial and perivascular inflammation. Even more strikingly, we found that an *in vivo* TLR4 antagonist given via the airways was likewise able to inhibit these features, including bronchial hyperreactivity to metacholine, an IL-13–dependent response[39].

Although endotoxin has long been held responsible for determining the development and severity of asthma[13,20], our data show that these effects occur mainly through TLR4 triggering of lung structural cells, thus driving activation of the mucosal DC network.

METHODS

Mice. We obtained *Tlr4*-deficient mice[40] from The Jackson Laboratory. MHCII-EGFP knock-in mice[41] were provided by H. Ploegh. All other mice were on the C57BL/6 background were obtained from Harlan and handled according to US National Institutes of Health institutional guidelines and guidelines of Ghent University. All experiments were approved by the Animal Ethical Committee of Ghent University. OTII mice on a *Rag1*$^{-/-}$–*Rag2*$^{-/-}$ background were from Taconic.

Construction of bone marrow chimeras. We sublethally irradiated 3–5-week-old *Tlr4*-deficient or WT recipient mice with 900 rad. On the same day, we collected 5×10^4 bone marrow cells from MHCII-EGFP mice (WT for TLR4) or *Tlr4*$^{-/-}$ mice and infused via the tail vein. For the imaging experiments, we used MHCII-EGFP mice on a *Rag1*$^{-/-}$*Rag2*$^{-/-}$ background (no B and T cells) as bone marrow donors. We kept these mice in isolators and provided neomycin-containing water until we used them 10–12 weeks later. To permit complete chimerism in the lung, we allowed 10–12 weeks of reconstitution time before we started experiments[42]; we confirmed the degree of chimerism of CD19$^+$MHCII$^+$ B cells, CD11c$^+$MHCII$^+$ DCs and alveolar macrophages, known to be slowly repopulated after irradiation, by measuring GFP positivity after 12 weeks of chimerism or by immunostaining of TLR4 expression on cryosections of lungs, followed by confocal imaging.

Reagents. We obtained allophycocyanin-labeled antibody to CD11c, phycoerythrin-labeled antibodies to CD11b and CD86 and biotinylated antibodies to Ly6C and 7-AAD from BD Biosciences. We obtained ultrapure preparations of LPS and peptidoglycan as well as the TLR4 antagonist (*R. sphaeroides* ultrapure LPS) from Invivogen. We obtained endotoxin-free OVA from Seikagaku, HDM extracts from Greer Laboratories, OVA labeled with Alexa Fluor 647 from Invitrogen and TLR4-specific antibodies from Santa Cruz.

Intratracheal administration of reagents. We anesthetized mice with isoflurane and administered 80 µl of PBS, LPS (10 µg or 100 ng per mouse), PGN (10 µg per mouse), HDM (100 µg per mouse) or TLR4 antagonist (1 µg per mouse) i.t.[43]

Immune analysis. We performed BAL by injecting 1 ml of PBS containing 0.01 mM EDTA. We collected the thoracic draining lymph nodes, lungs and trachea and prepared single-cell suspensions as previously reported[2]. We stained cell suspensions in PBS supplemented with 2 mM EDTA, 0.5% BSA and 0.01% sodium azide. We obtained monoclonal antibodies (conjugated to various fluorochromes or biotin) and fluorescence-labeled streptavidin from BD Biosciences. We used 2.4G2 (antibody to Fcγ receptor III/II) to block unspecific antibody binding. We stained single-cell suspensions with FITC-labeled antibody to MHC class II, phycoerythrin-labeled antibody to CD40, phycoerythrin-labeled antibody to CD80, phycoerythrin-labeled antibody to CD86 and allophycocyanin-labeled anti-CD11c antibodies (all from BD Biosciences). We collected data on a FACSCalibur (Becton Dickinson) analyzed it with FlowJo software (Treestar).

To measure cytokine concentrations, we plated MLN cells in round bottom 96-well plates (1 × 106 cells per ml) and re-stimulated them with HDM extracts (30 µg ml^{-1}) for 5 d. Then we collected the culture supernatant and assayed it by commercially available ELISA (R&D Systems).

House dust mite–induced airway inflammation. We exposed mice to *Dermatophagoides pteronyssinus* extracts (Greer Laboratories, 10.52 endotoxin units per mg endotoxin) via i.t. injection of HDM (100 µg) on days 0, 7 and 14 and analyzed them on day 17. We performed BAL and analyzed the cells by flow cytometry as previously described[44]. We stained lung slides with periodic acid Schiff. We measured lung function by Flexivent invasive measurement of dynamic resistance as previously described[45].

Preparation of explants. We injected mice i.t. with LPS or PBS 2 h before we killed them by CO_2 asphyxiation. We stained the tracheal explant with 100 µM SNARF (Invitrogen) for 10 s at 37 °C in PBS. We then immobilized the trachea on the surface of a Petri dish with Vetbond epoxy glue (3M Animal Care Products) and a mechanical support, and we submerged the entire preparation in 20 ml of phenol red–free RPMI maintained at 37 °C. During microscopy, we superfused the medium with a gas mixture of 95% O_2 and 5% CO_2.

Two-photon microscopy. We conducted two-photon microscopy with a Bio-Rad Laboratories Radiance 2100MP system equipped with a Nikon 600FN upright microscope, a 20× water immersion lens (numerical aperture 0.95; Olympus) and a Mira 900 Sa:Ti femtosecond-pulsed laser driven by a 10-W Verdi pump laser (Coherent) tuned to 880 nm. The typical pixel size of the image field was 1.09 µm, and the *x-y* dimensions of the scan area were 560 µm × 560 µm. The typical optical *z*-step size was 2 µm. We collected serial *x-y* images over the entire *z* depth every 30–60 s, and we repeated the entire process for up to 60 min to obtain a four-dimensional data set.

Image processing. We processed data sets with edge-preserving filters for the green channel and a median filter for the red and blue channels (Bitplane, 4.2; Imaris) to de-noise the images. We used the same software to color-balance the images, with all manipulations of color and intensity applied equally to an entire image stack, and we used the resulting files to create two-dimensional maximum intensity projections for the image stack corresponding to each time segment. We then combined these projections with Adobe After Effects to generate video sequences.

Statistical analyses. For all experiments, we calculated the difference between groups with the Mann-Whitney *U* test for unpaired data (GraphPad Prism version 4.0; GraphPad Software). Differences were considered significant when $P < 0.05$.

Additional methods. Detailed methodology is described in the **Supplementary Methods** online.

Note: Supplementary information is available on the Nature Medicine website.

ACKNOWLEDGMENTS
MHCII-EGFP knock-in mice were provided by H. Ploegh (Harvard Medical School). B.N.L. is a recipient of an Odysseus grant from the Flemish government. We wish to thank T. Boterberg for help with mouse irradiation and S. De Prijck and M. Van Heerswinghel for help with experiments.

AUTHOR CONTRIBUTIONS
H.H., M.C., M.A.W. and F.P. performed and analyzed experiments; M.C. and R.N.G. were instrumental in setting up the live dual-photon imaging; R.N.G. supervised the work at the US National Institutes of Health and B.N.L. supervised the work at Ghent University. All authors contributed collectively to the conception of the project, to the planning, discussion and interpretation of experiments, and to the writing of the paper.

Published online at http://www.nature.com/naturemedicine/
Reprints and permissions information is available online at http://npg.nature.com/reprintsandpermissions/

1. Barnes, P.J. Immunology of asthma and chronic obstructive pulmonary disease. *Nat. Rev. Immunol.* **8**, 183–192 (2008).

© 2009 Nature America, Inc. All rights reserved.

2. Vermaelen, K.Y., Carro-Muino, I., Lambrecht, B.N. & Pauwels, R.A. Specific migratory dendritic cells rapidly transport antigen from the airways to the thoracic lymph nodes. *J. Exp. Med.* **193**, 51–60 (2001).
3. Stampfli, M.R. *et al.* GM-CSF transgene expression in the airway allows aerosolized ovalbumin to induce allergic sensitization in mice. *J. Clin. Invest.* **102**, 1704–1714 (1998).
4. Ziegler, S.F. & Liu, Y.J. Thymic stromal lymphopoietin in normal and pathogenic T cell development and function. *Nat. Immunol.* **7**, 709–714 (2006).
5. Sha, Q. *et al.* Activation of airway epithelial cells by Toll-like receptor agonists. *Am. J. Respir. Cell Mol. Biol.* **31**, 358–364 (2004).
6. Guillot, L. *et al.* Response of human pulmonary epithelial cells to lipopolysaccharide involves Toll-like receptor 4 (TLR4)-dependent signaling pathways: evidence for an intracellular compartmentalization of TLR4. *J. Biol. Chem.* **279**, 2712–2718 (2004).
7. Skerrett, S.J. *et al.* Respiratory epithelial cells regulate lung inflammation in response to inhaled endotoxin. *Am. J. Physiol. Lung Cell. Mol. Physiol.* **287**, L143–L152 (2004).
8. Hammad, H. & Lambrecht, B.N. Dendritic cells and epithelial cells: linking innate and adaptive immunity in asthma. *Nat. Rev. Immunol.* **8**, 193–204 (2008).
9. Saito, T. *et al.* Expression of Toll-like receptor 2 and 4 in lipopolysaccharide-induced lung injury in mouse. *Cell Tissue Res.* **321**, 75–88 (2005).
10. Berndt, A. *et al.* Elevated amount of Toll-like receptor 4 mRNA in bronchial epithelial cells is associated with airway inflammation in horses with recurrent airway obstruction. *Am. J. Physiol. Lung Cell. Mol. Physiol.* **292**, L936–L943 (2007).
11. Trompette, A. *et al.* Allergenicity resulting from functional mimicry of a Toll-like receptor complex protein. *Nature* **457**, 585–588 (2009).
12. Reis E Sousa, C. Dendritic cells in a mature age. *Nat. Rev. Immunol.* **6**, 476–483 (2006).
13. Braun-Fahrlander, C. *et al.* Environmental exposure to endotoxin and its relation to asthma in school-age children. *N. Engl. J. Med.* **347**, 869–877 (2002).
14. Lewkowich, I.P. *et al.* $CD4^+CD25^+$ T cells protect against experimentally induced asthma and alter pulmonary dendritic cell phenotype and function. *J. Exp. Med.* **202**, 1549–1561 (2005).
15. Fattouh, R. *et al.* House dust mite facilitates ovalbumin-specific allergic sensitization and airway inflammation. *Am. J. Respir. Crit. Care Med.* **172**, 314–321 (2005).
16. Cates, E.C. *et al.* Intranasal exposure of mice to house dust mite elicits allergic airway inflammation via a GM-CSF–mediated mechanism. *J. Immunol.* **173**, 6384–6392 (2004).
17. Fallon, P.G. *et al.* Identification of an interleukin (IL)-25–dependent cell population that provides IL-4, IL-5, and IL-13 at the onset of helminth expulsion. *J. Exp. Med.* **203**, 1105–1116 (2006).
18. Kondo, Y. *et al.* Administration of IL-33 induces airway hyperresponsiveness and goblet cell hyperplasia in the lungs in the absence of adaptive immune system. *Int. Immunol.* **20**, 791–800 (2008).
19. Zhou, B. *et al.* Thymic stromal lymphopoietin as a key initiator of allergic airway inflammation in mice. *Nat. Immunol.* **6**, 1047–1053 (2005).
20. Eisenbarth, S.C. *et al.* Lipopolysaccharide-enhanced, Toll-like receptor 4-dependent T helper cell type 2 responses to inhaled antigen. *J. Exp. Med.* **196**, 1645–1651 (2002).
21. Nolte, M.A., Leibundgut-Landmann, S., Joffre, O. & Sousa, C.R. Dendritic cell quiescence during systemic inflammation driven by LPS stimulation of radioresistant cells in vivo. *J. Exp. Med.* **204**, 1487–1501 (2007).
22. Poynter, M.E., Irvin, C.G. & Janssen-Heininger, Y.M. A prominent role for airway epithelial NF-κB activation in lipopolysaccharide-induced airway inflammation. *J. Immunol.* **170**, 6257–6265 (2003).
23. Noulin, N. *et al.* Both hematopoietic and resident cells are required for MyD88-dependent pulmonary inflammatory response to inhaled endotoxin. *J. Immunol.* **175**, 6861–6869 (2005).
24. Lorenz, E. *et al.* Genes other than TLR4 are involved in the response to inhaled LPS. *Am. J. Physiol. Lung Cell. Mol. Physiol.* **281**, L1106–L1114 (2001).
25. Pichavant, M. *et al.* Asthmatic bronchial epithelium activated by the proteolytic allergen Der p 1 increases selective dendritic cell recruitment. *J. Allergy Clin. Immunol.* **115**, 771–778 (2005).
26. Nathan, A.T., Peterson, E.A., Chakir, J. & Wills-Karp, M. Innate immune responses of airway epithelium to house dust mite are mediated through β-glucan–dependent pathways. *J. Allergy Clin. Immunol.* published online, doi:10.1016/j.jaci.2008.12.006 (27 January 2009).
27. Robays, L.J. *et al.* Chemokine receptor CCR2 but not CCR5 or CCR6 mediates the increase in pulmonary dendritic cells during allergic airway inflammation. *J. Immunol.* **178**, 5305–5311 (2007).
28. Geissmann, F., Jung, S. & Littman, D.R. Blood monocytes consist of two principal subsets with distinct migratory properties. *Immunity* **19**, 71–82 (2003).
29. Veres, T.Z. *et al* Spatial interactions between dendritic cells and sensory nerves in allergic airway inflammation. *Am. J. Respir. Cell Mol. Biol.* **37**, 553–561 (2007).
30. Bajenoff, M. *et al.* Stromal cell networks regulate lymphocyte entry, migration and territoriality in lymph nodes. *Immunity* **25**, 989–1001 (2006).
31. Hammad, H. & Lambrecht, B.N. Lung dendritic cell migration. *Adv. Immunol.* **93**, 265–278 (2007).
32. Stumbles, P.A. *et al.* Resting respiratory tract dendritic cells preferentially stimulate T helper cell type 2 (T_H2) responses and require obligatory cytokine signals for induction of T_H1 immunity. *J. Exp. Med.* **188**, 2019–2031 (1998).
33. Bilyk, N. & Holt, P.G. Inhibition of the immunosuppressive activity of resident pulmonary alveolar macrophages by granulocyte/macrophage colony–stimulating factor. *J. Exp. Med.* **177**, 1773–1777 (1993).
34. Piggott, D.A. *et al.* MyD88-dependent induction of allergic T_H2 responses to intranasal antigen. *J. Clin. Invest.* **115**, 459–467 (2005).
35. Liu, Y.J. Thymic stromal lymphopoietin: master switch for allergic inflammation. *J. Exp. Med.* **203**, 269–273 (2006).
36. Angkasekwinai, P. *et al.* Interleukin 25 promotes the initiation of proallergic type 2 responses. *J. Exp. Med.* **204**, 1509–1517 (2007).
37. Sokol, C.L., Barton, G.M., Farr, A.G. & Medzhitov, R. A mechanism for the initiation of allergen-induced T helper type 2 responses. *Nat. Immunol.* **9**, 310–318 (2008).
38. Schmitz, J. *et al.* IL-33, an interleukin-1–like cytokine that signals via the IL-1 receptor–related protein ST2 and induces T helper type 2–associated cytokines. *Immunity* **23**, 479–490 (2005).
39. Wills-Karp, M. *et al.* Interleukin-13: central mediator of allergic asthma. *Science* **282**, 2258–2261 (1998).
40. Beutler, B. & Poltorak, A. The sole gateway to endotoxin response: how LPS was identified as Tlr4, and its role in innate immunity. *Drug Metab. Dispos.* **29**, 474–478 (2001).
41. Boes, M. *et al.* T-cell engagement of dendritic cells rapidly rearranges MHC class II transport. *Nature* **418**, 983–988 (2002).
42. Matute-Bello, G. *et al.* Optimal timing to repopulation of resident alveolar macrophages with donor cells following total body irradiation and bone marrow transplantation in mice. *J. Immunol. Methods* **292**, 25–34 (2004).
43. Lambrecht, B.N., Salomon, B., Klatzmann, D. & Pauwels, R.A. Dendritic cells are required for the development of chronic eosinophilic airway inflammation in response to inhaled antigen in sensitized mice. *J. Immunol.* **160**, 4090–4097 (1998).
44. Van Rijt, L.S. *et al.* A rapid flow cytometric method for determining the cellular composition of bronchoalveolar lavage fluid cells in mouse models of asthma. *J. Immunol. Methods* **288**, 111–121 (2004).
45. Hammad, H. *et al.* Activation of the D prostanoid 1 receptor suppresses asthma by modulation of lung dendritic cell function and induction of regulatory T cells. *J. Exp. Med.* **204**, 357–367 (2007).

© 2009 Nature America, Inc. All rights reserved.

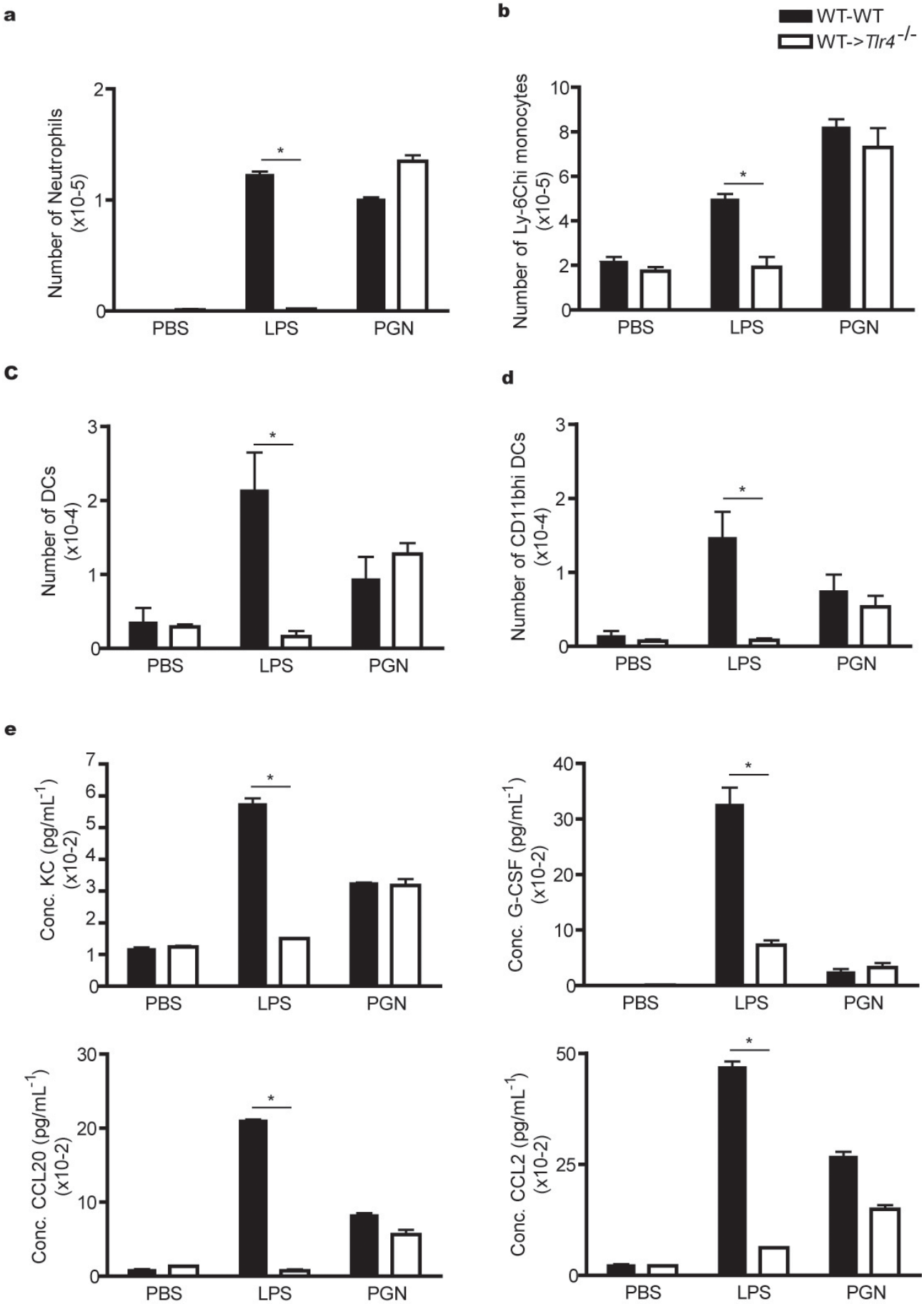

Supplementary Figure 1

Nature Medicine: doi:10.1038/nm.1946

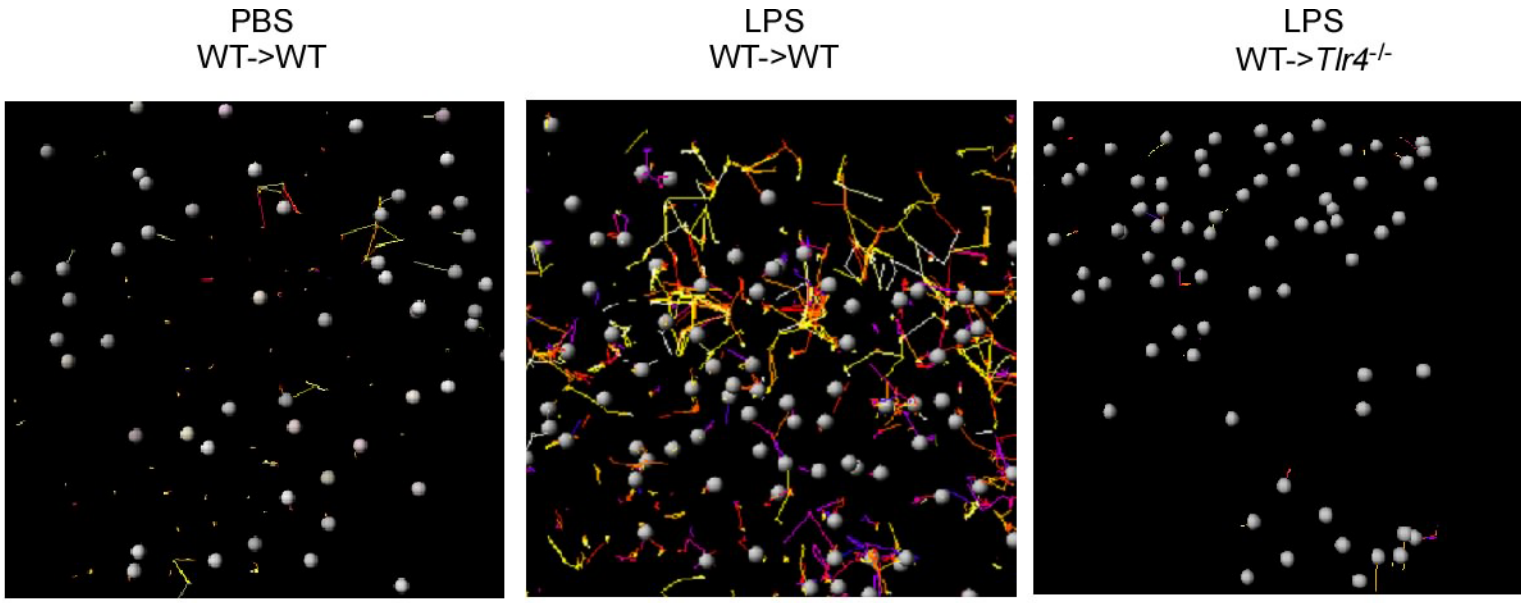

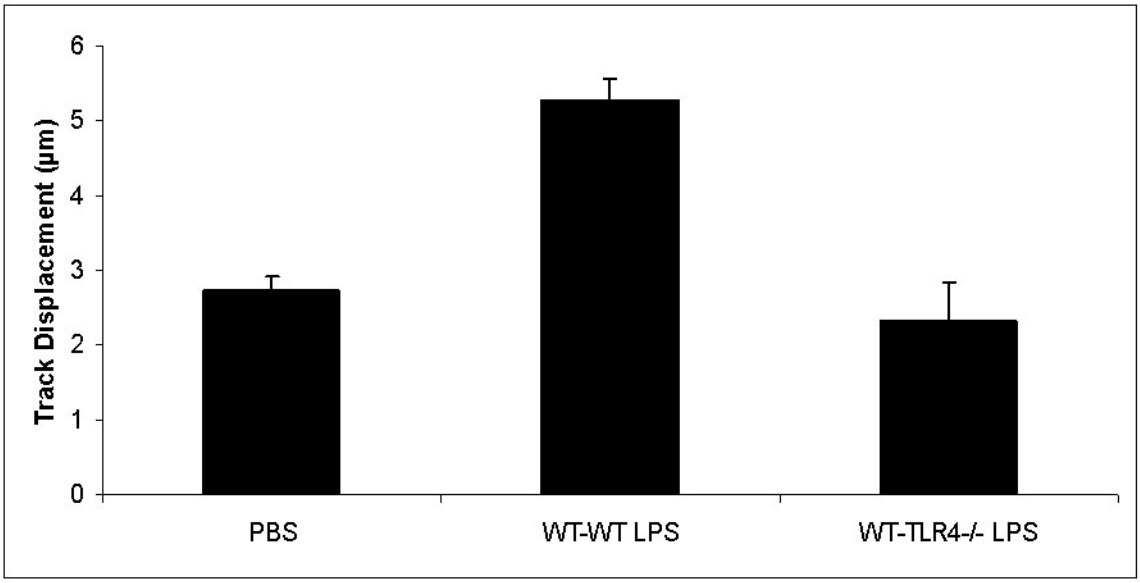

Nature Medicine: doi:10.1038/nm.1946

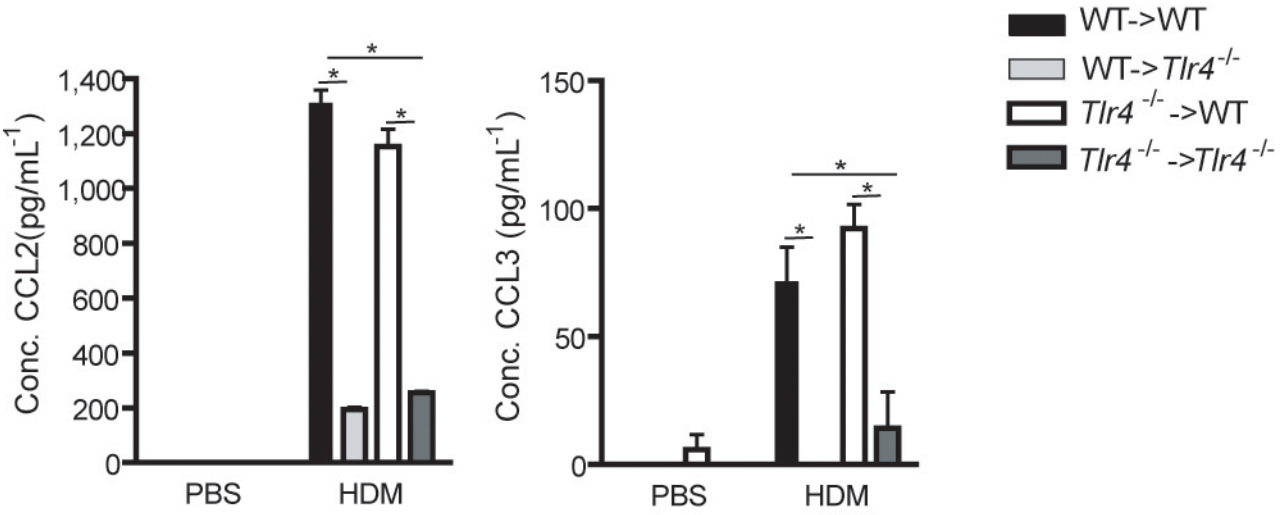

Supplementary Figure 3

Nature Medicine: doi:10.1038/nm.1946

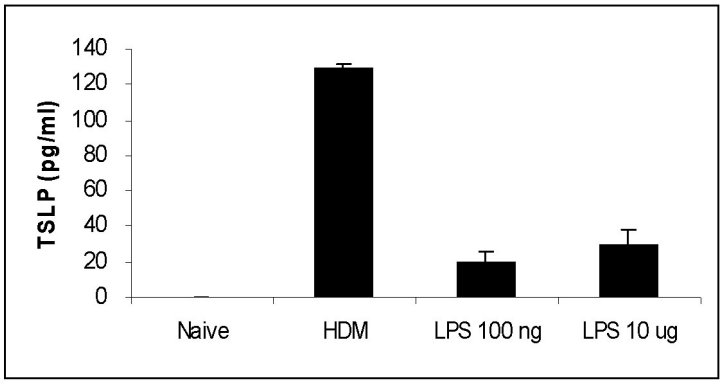

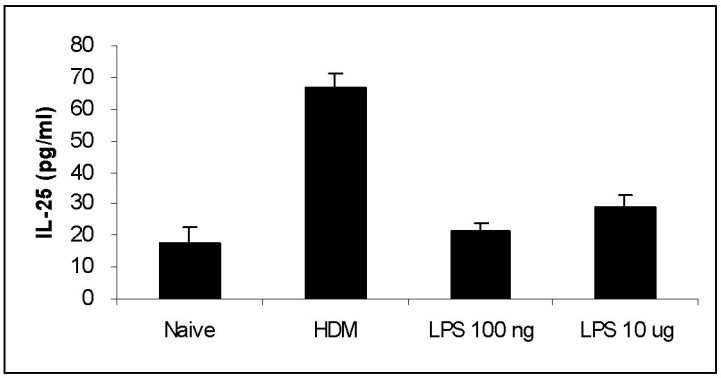

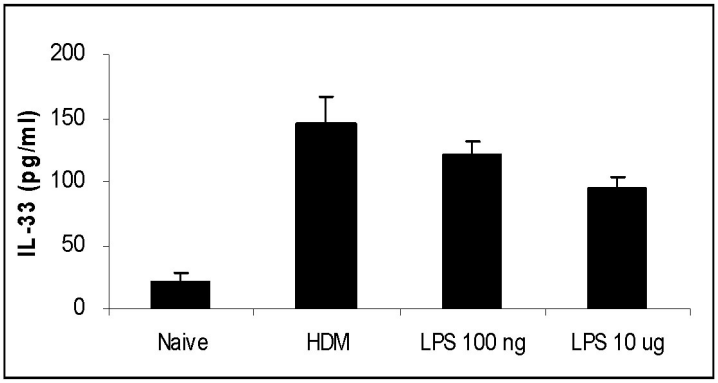

Nature Medicine: doi:10.1038/nm.1946

	MFI CD86	***MFI CD40***
WT◊WT	3.3±0.76	3.8±0.27
WT◊ *Tlr4*$^{-/-}$	1.22±0.38	1.86±0.21
Tlr4$^{-/}$◊WT	3.7±0.65	2.98±0.54
Tlr4$^{-/-}$◊ *Tlr4*$^{-/-}$	1.17±0.27	1.31±0.39

Supplementary Table 1

Supplementary online data

Supplementary movie 1: In situ behaviour of non-stimulated airway DCs. Video of a tracheal explant from a WT->WT mouse given *PBS* intratracheally. The trachea was explanted, stained with Hoechst (blue) and immobilized. Total time, 26 min. Playback speed, 120x. Bar, 70 µm.

Supplementary movie 2: In situ behaviour of LPS-activated airway DCs in WT->WT chimeric mice. Video of a tracheal explant from a WT->WT chimeric mouse given *LPS* intratracheally. The trachea was explanted, stained with Hoechst (blue) and immobilized. Total time, 26 min. Playback speed, 120x. Bar, 70 µm.

Supplementary movie 3: In situ behaviour of LPS-activated airway DCs in WT->TLR4-/- chimeric mice. Video of a tracheal explant from an MHCII-EGFP mouse given *LPS* intratracheally. The trachea was explanted, stained with Hoechst (blue) and immobilized. Total time, 26 min. Playback speed, 120x. Bar, 70 µm.

Supplementary Figure 1: Recruitment of immune cells to the lungs in response to PGN is intact in WT->TLR4$^{-/-}$ chimeras. WT->WT and WT->TLR4$^{-/-}$ chimeras were injected i.t with LPS, PGN, or PBS. The recruitment of (A) neutrophils, (B) monocytes, (C) MHCII+CD11c+ dendritic cells and (D) MHCII+CD11c+CD11b+ DCs was analyzed. (E) Chemokine production in BAL fluids. *:$p<0.05$.

Supplementary Figure 2

Quantification of movements of MHCII^{eGfp} DCs in tracheal explants. Mice were treated *in vivo* with PBS or LPS and tracheal explants were made 2h later.

Tracks of individual cells in the X-Y-Z space over time were calculated using Imaris 5.0 software package. This experiment was performed in WT->WT and WT->TLR4 chimeric mice. Bar histograms represent the average length of the displacement tracks.

Supplementary figure 3:

TLR4 expression on airway structural cells is necessary and sufficient for chemokine production in the airways in response to HDM allergen. Chimeras were injected i.t with PBS or HDM allergen. Production of CCL2 (A), and CCL3 (B) was measured in BAL fluids 24 hours later. *:$p<0.05$. This is one representative experiment out of 3. 5-6 mice /group were used.

Supplementary Figure 4

Comparison of production of innate proallergic cytokines following administration of LPS or HDM. Mice received an intratracheal injection of 100 µg of HDM, 100 ng LPS or 10 µg of LPS. Thirty-six h later, the levels of TSLP, IL-25 and IL-33 were measured in the BAL fluid.

Supplementary table 1

Table summarizing the induction of MFI intensity of CD86 and CD40 expression on $CD11c^+$ tracheal DC subsets 24h following *in vivo* exposure to LPS (fold induction over PBS exposure).